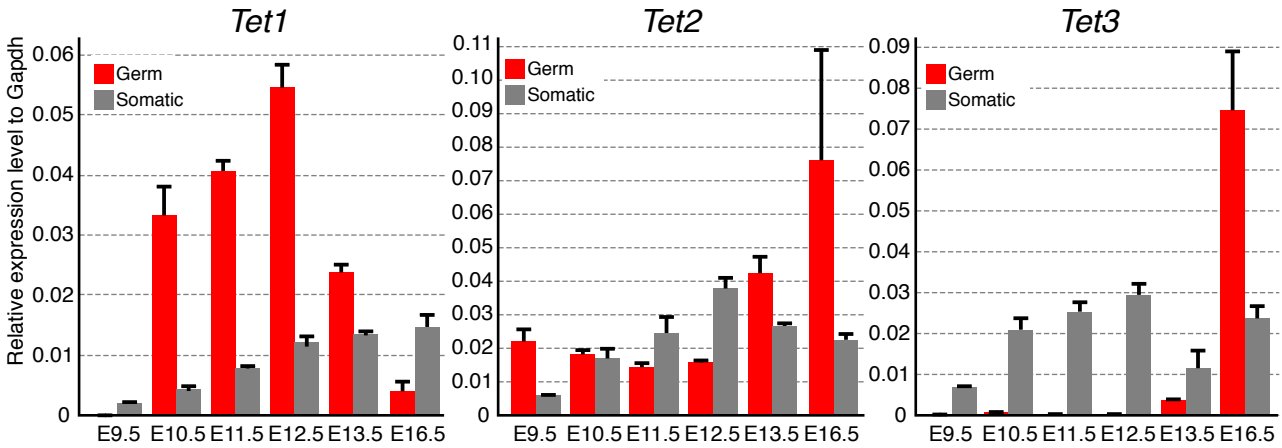

Figure S1. Expression levels of Tet transcripts in PGCs and adjacent somatic cells during embryonic development

RT-qPCR analysis of the gene expression levels of Tet genes during germ cell development. The Ct values were normalized to the expression level of Gapdh. PGCs were purified by FACS based on GOF18ΔPE-EGFP transgene expression.

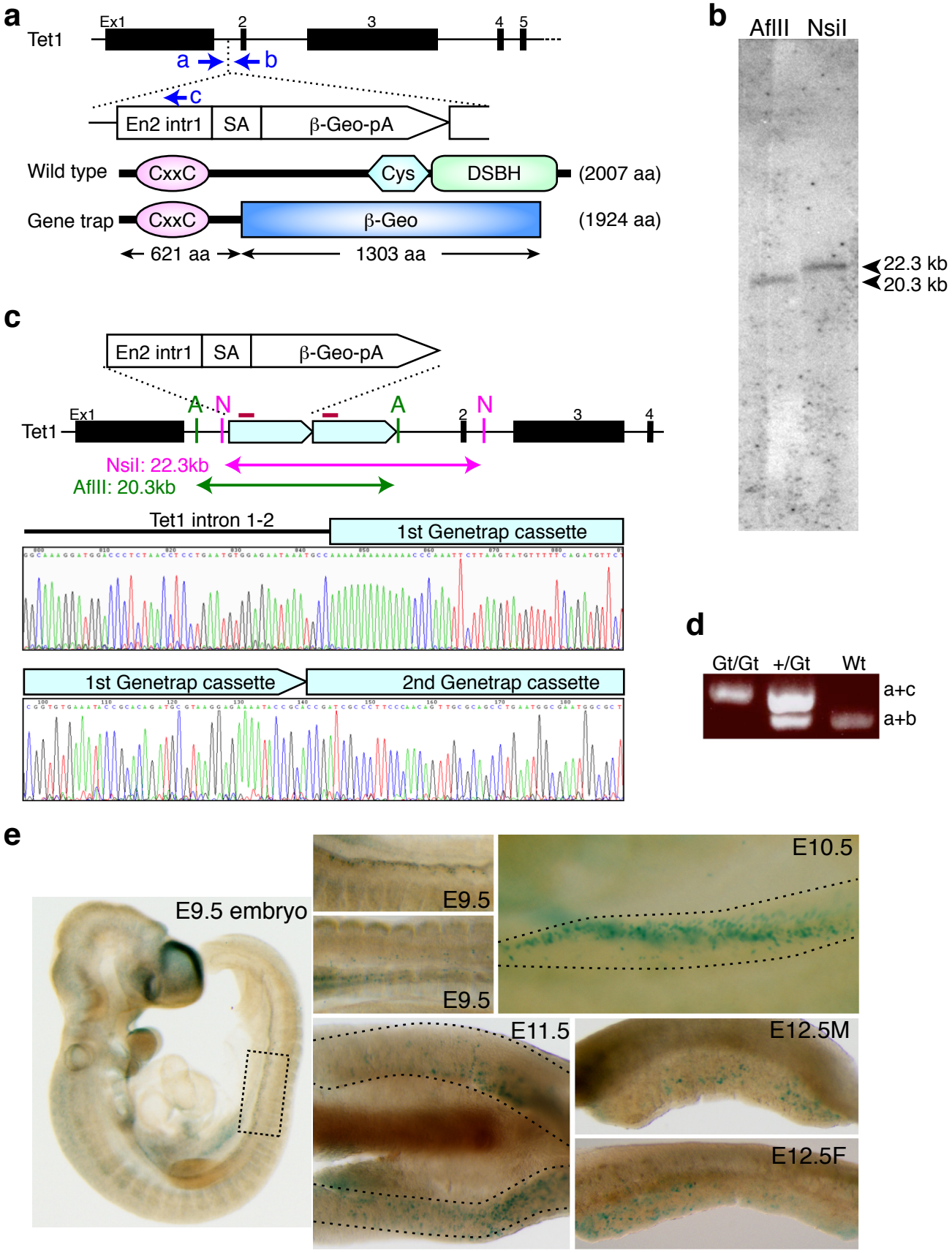
a
Tet1
Ex1
2
3
4
5
a
b
c
En2 intr1
SA
β-Geo-pA
Wild type
CxxC
Cys
DSBH
(2007 aa)
Gene trap
CxxC
β-Geo
(1924 aa)
621 aa
1303 aa
b
AflII
NsiI
22.3 kb
20.3 kb
c
En2 intr1
SA
β-Geo-pA
A
N
A
N
Ex1
Tet1
2
3
4
NsiI: 22.3kb
AflII: 20.3kb
Tet1 intron 1-2
1st Genetrap cassette
1st Genetrap cassette
2nd Genetrap cassette
d
Gt/Gt
+/Gt
Wt
a+c
a+b
e
E9.5 embryo
E9.5
E9.5
E10.5
E11.5
E12.5M
E12.5F

Figure S2. Confirmation of correct insertion of gene-trap cassette into the Tet1 locus
(a) Schematic diagram of Tet1-gene-trap cassette. Upper panel, Tet1 locus and inserted gene cassette. SA: splicing acceptor, En2: engrailed homolog 2, β-Geo: β-garactosidase+Neo^r fusion gene, pA: polyadenylation signal. Bottom panel, Schematic diagram of the protein products from both the wild-type and gene-trap alleles. Cys: cystein-rich region, DSBH: double stranded β-helix domain.
(b) Southern blot analysis demonstrating a single locus insertion into the Tet1-Gt mouse using an internal probe. The location of the probe and the expected size of the digested fragments are indicated in the diagram in panel c.
(c) Upper panel, schematic diagram of the inserted repeated Tet1-gene-trap cassette. Bottom panel, genomic sequencing confirmation of the tandem insertion of two copies of gene trap cassettes into a single locus.
(d) EtBr-stained agarose gel containing genomic PCR products for genotyping. The locations of PCR primers are indicated in panel a.
(e) X–gal staining of E9.5 to E12.5 embryos demonstrates PGC-specific expression of the gene-trap cassette. Genital ridges are indicated by dashed lines.

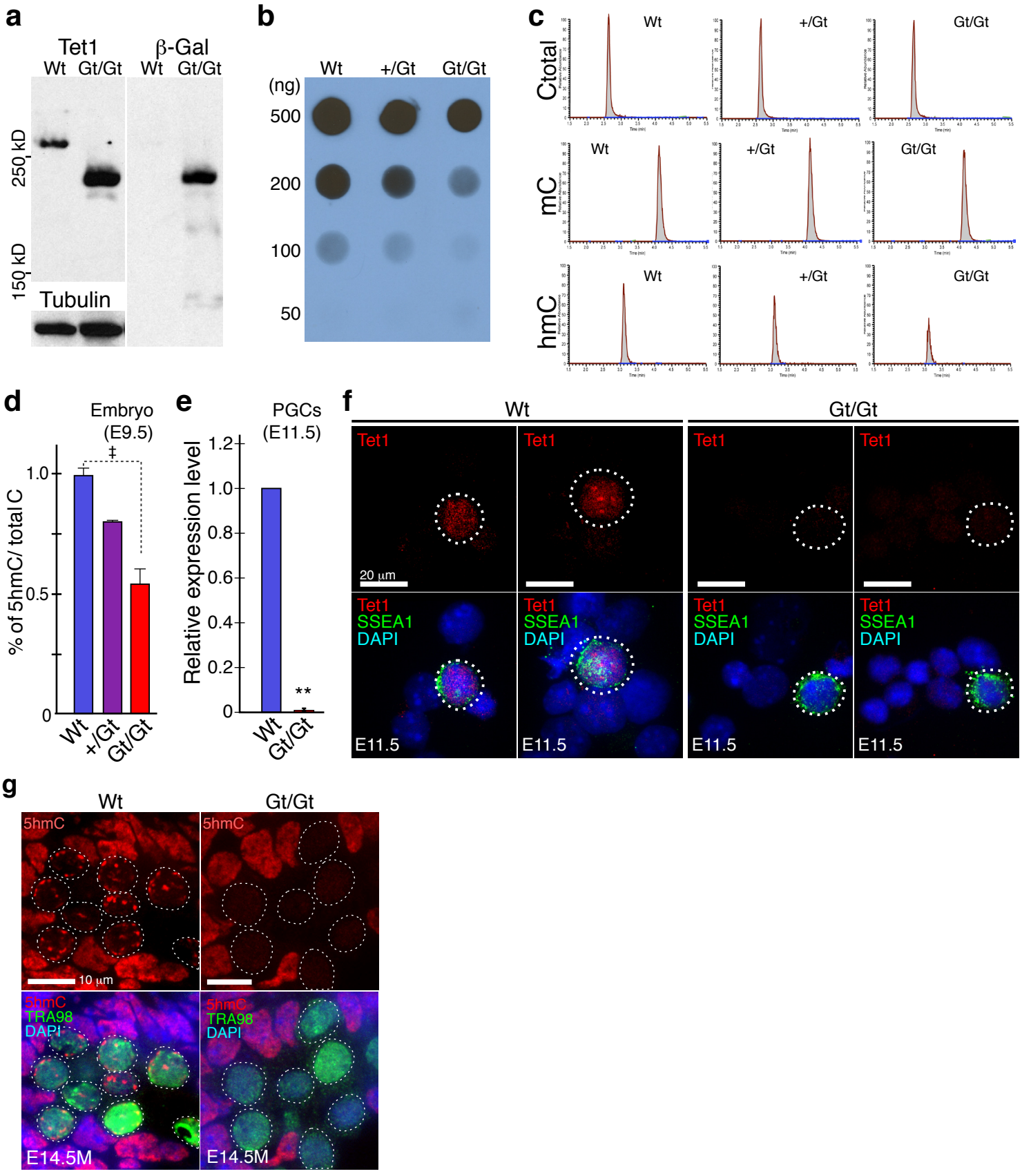
a
Tet1
β-Gal
Wt Gt/Gt Wt Gt/Gt
250 kD
150 kD
Tubulin
b
Wt +/Gt Gt/Gt
(ng)
500
200
100
50
c
Ctotal
mC
hmC
Wt
+/Gt
Gt/Gt
d
Embryo
(E9.5)
% of 5hmC/ total C
1.0
0.5
0
Wt
+/Gt
Gt/Gt
e
PGCs
(E11.5)
Relative expression level
1.2
1.0
0.8
0.6
0.4
0.2
0
**
Wt
Gt/Gt
f
Wt
Gt/Gt
Tet1
20 μm
Tet1
SSEA1
DAPI
E11.5
g
Wt
Gt/Gt
5hmC
10 μm
5hmC
TRA98
DAPI
E14.5M

Figure S3. Loss of Tet1 expression and 5hmC in PGCs of the Tet1$^{Gt/Gt}$ mice
(a) Western blot analysis of wild-type and Tet1$^{Gt/Gt}$ ES cell extracts with anti-Tet1, anti-βGal, and anti-Tubulin antibodies. Tubulin serves as a loading control. The 150 and 250 kDa protein size marks are indicated. The band above the 250 kDa size mark is Tet1 and the band below the 250 kDa mark is the Tet1(aa1-621)-β–Gal fusion protein.
(b) Dot blot analysis of the genomic 5hmC levels in E9.5 embryos of wild-type (Wt), heterozygous (+/Gt), and homozygous (Gt/Gt) mice. The amount of genomic DNA in each spot is indicated.
(c, d) The original Mass spectrometric data (c) and quantification (d) of genomic 5hmC levels in E9.5 embryos of wild-type (Wt), heterozygous (+/Gt), and homozygous (Gt/Gt) mice. The bars represent the average of three independent experiments with standard deviation. ‡P=0.059.
(e) RT-qPCR analysis of the Tet1 levels in E11.5 PGCs of wild-type (Wt) and homozygous (Gt/Gt) mice. The Tet1 expression level at Wt PGCs is normalized with Gapdh and is set as 1. **P<0.01.
(f) Representative images of E11.5 PGC spreads stained with Tet1 antibodies. SSEA1 serves as a mark for PGCs and is indicated by arrows.
(g) Immunostaining of E14.5 mouse genitor ridge cells with 5hmC antibodies (red). PGCs are indicated by dashed circles and are positive for TRA98 (green). Note that the doted 5hmC pattern in PGCs is lost in the Tet1Gt/Gt PGCs.

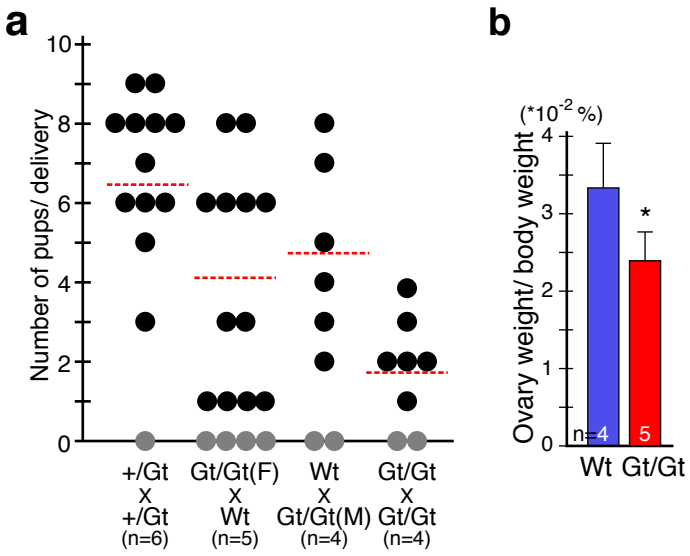

Figure S4. Reduction in the fertility and ovary size in Tet1$^{Gt/Gt}$ mice
(a) Mating scores of Tet1Gt/Gt mice. The number of pups of each litter is indicated by a black dot. Gray dot indicates observation of vaginal plug but no delivery. The mean litter size is indicated by a red dashed line. The number of mating pairs (genotypes are indicated) used for each mating group are indicated at the bottom.
(b) Relative ovary to body weight from 8-week-old wild-type (Wt) and Tet1 mutant (Gt/Gt) mice. n=4 or 5. Error bars indicate SEM. *P<0.05

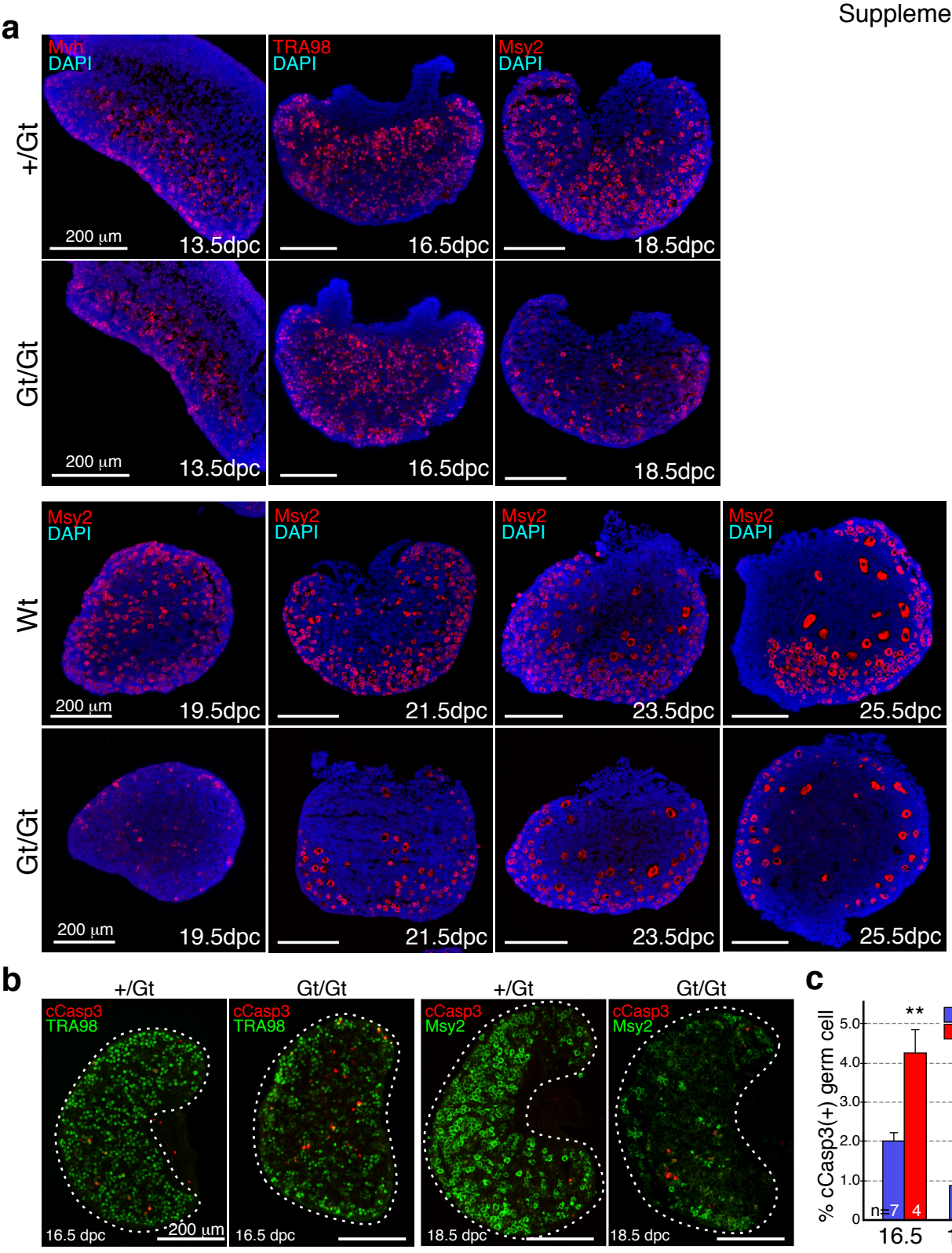

Figure S5. Germ cells loss in the Tet1$^{Gt/Gt}$ ovary

(a) Representative images of heterozygous (+/Gt), and homozygous (Gt/Gt) mouse embryonic and neonatal ovary sections stained with antibodies against germ cell markers Mvh, TRA98 and Msy2.

(b) Representative images of E16.5 and E18.5 ovary sections of Tet1$^{+/Gt}$ and Tet1$^{Gt/Gt}$ mice co-stained with germ cell marker TRA98, Msy2 and apoptotic marker cleaved-Caspase 3 (cCasp3).

(c) Percentage of apoptotic germ cells in E16.5 and E18.5 ovaries of Tet1$^{+/Gt}$ and Tet1$^{Gt/Gt}$ mice. n=4-7. Error bars indicate SEM. **P<0.01.

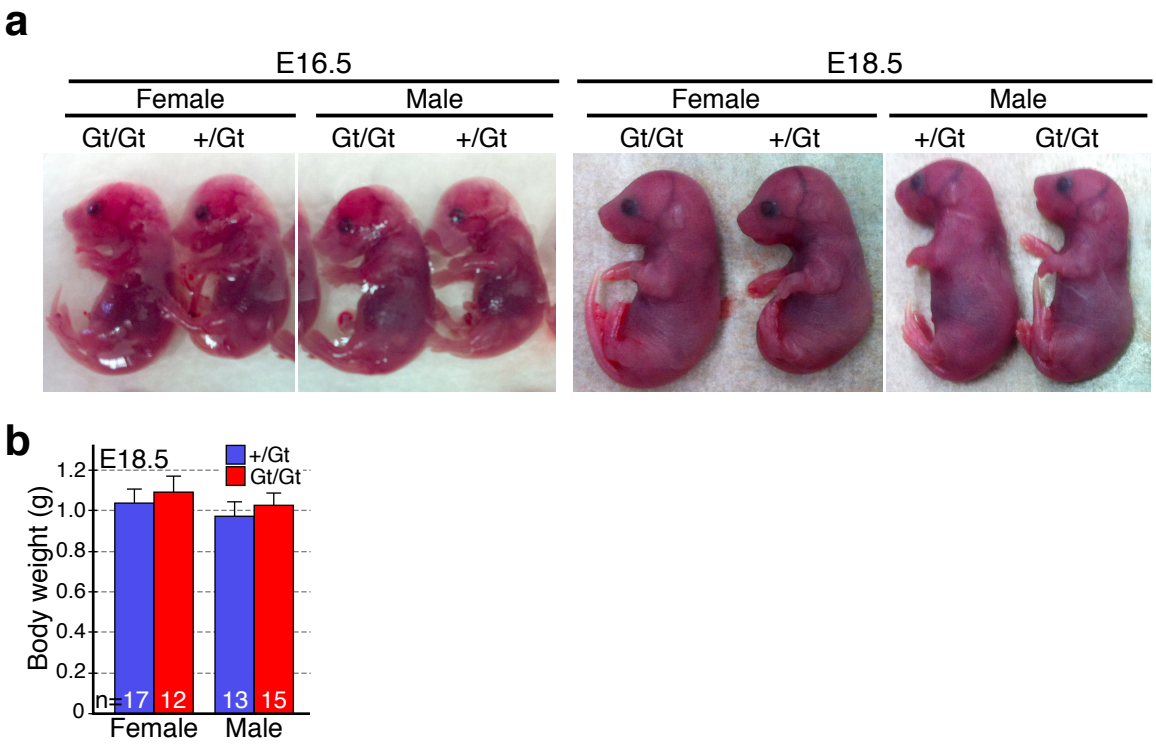

Figure S6. No significant difference in the size of embryo between Tet1$^{+/Gt}$ and Tet1$^{Gt/Gt}$

(a) Representative images of E16.5 and E18.5 Tet1$^{+/Gt}$ and Tet1$^{Gt/Gt}$ embryos.
(b) Average body weight of E18.5 Tet1$^{+/Gt}$ and Tet1$^{Gt/Gt}$ embryos. Error bar indicates SEM. n=12-17.

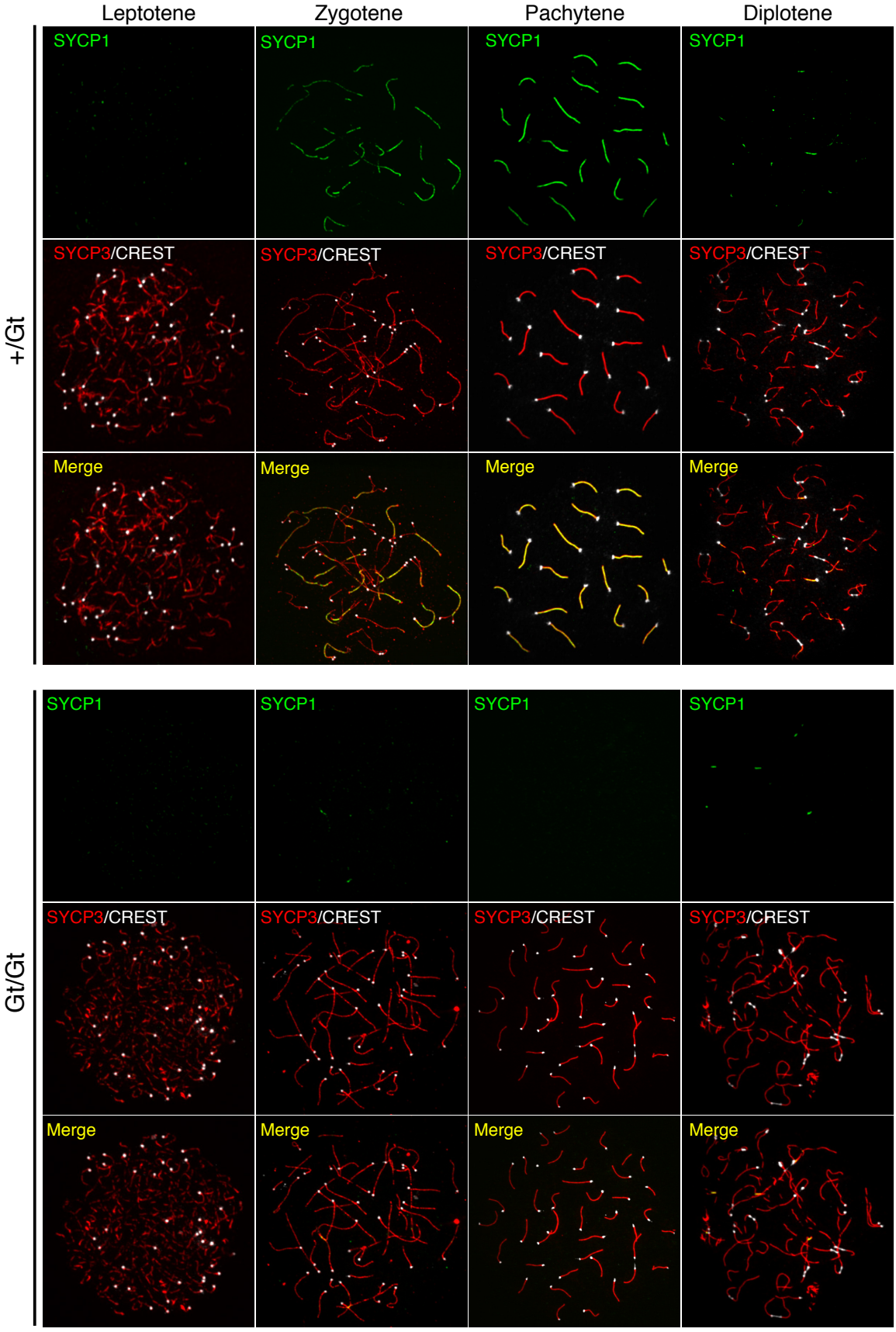

Figure S7. Synapsis defect in Tet1$^{Gt/Gt}$ oocytes
Representative images of oocytes stained with antibodies against SYCP1, SYCP3, and CREST. Note that the majority of the SYCP3-positive axial elements failed to align and SYCP1 signal is not detected in Tet1$^{Gt/Gt}$ oocytes at both zygotene and pachytene stage oocytes.

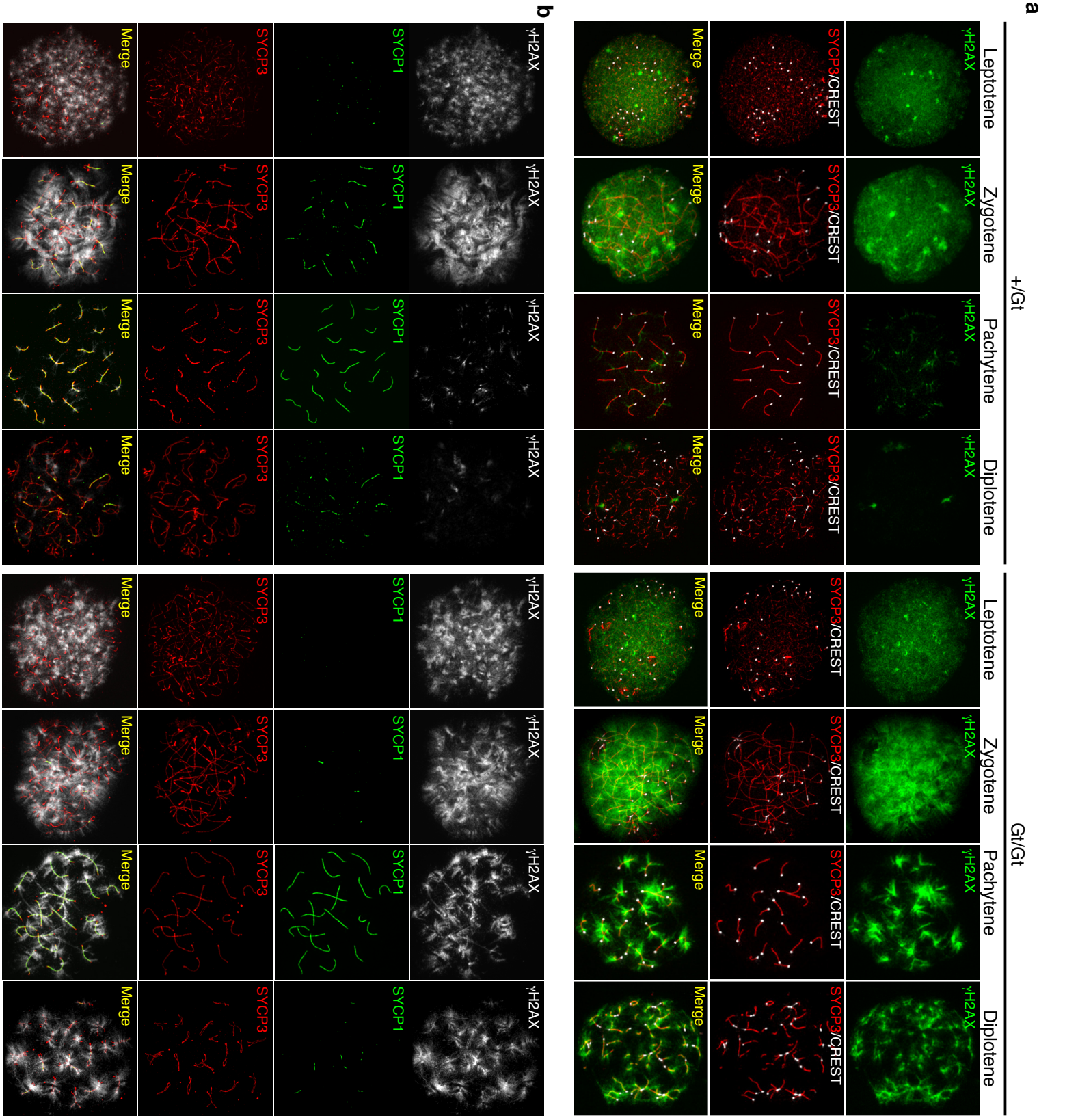

Figure S8. Accumulation of γH2AX in pachytene and diplotene Tet1$^{Gt/Gt}$ oocytes
(a) Representative images of meiotic Tet1$^{+/Gt}$ and Tet1$^{Gt/Gt}$ oocytes co-stained with γH2AX, SYCP3, and CREST antibodies.
(b) Representative images of meiotic Tet1$^{+/Gt}$ and Tet1$^{Gt/Gt}$ oocytes co-stained with γH2AX, SYCP3, and SYCP1 antibodies.

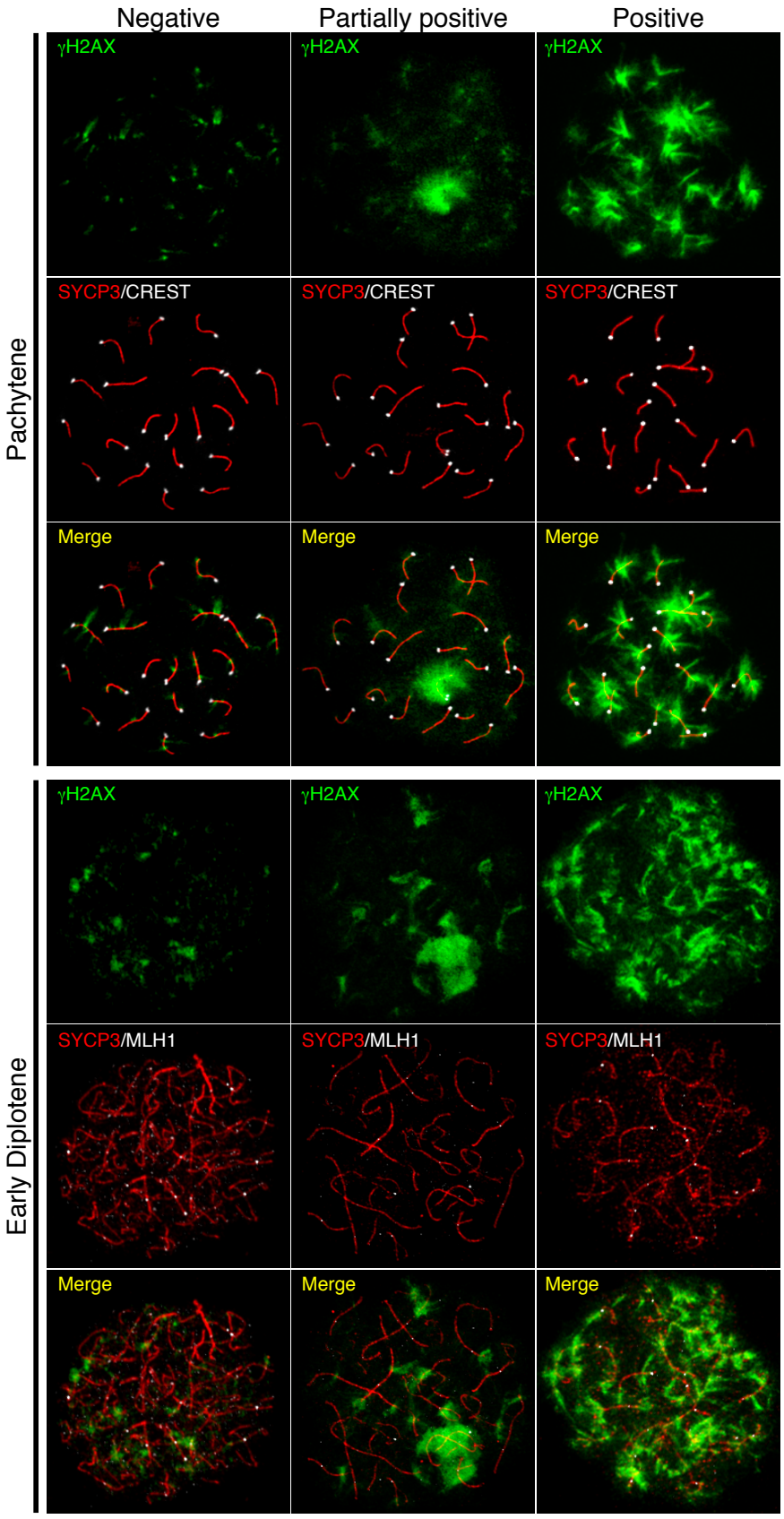

Figure S9. Classification of pachytene and early diplotene oocytes based on the level of γH2AX accumulation

Representative images of pachytene and early diplotene oocytes classified based on the level of γH2AX accumulation. Meiotic oocytes were co-stained with γH2AX, SYCP3, and CREST (pachytene stage), or γH2AX, SYCP3, and MLH1 (early diplotene stage).

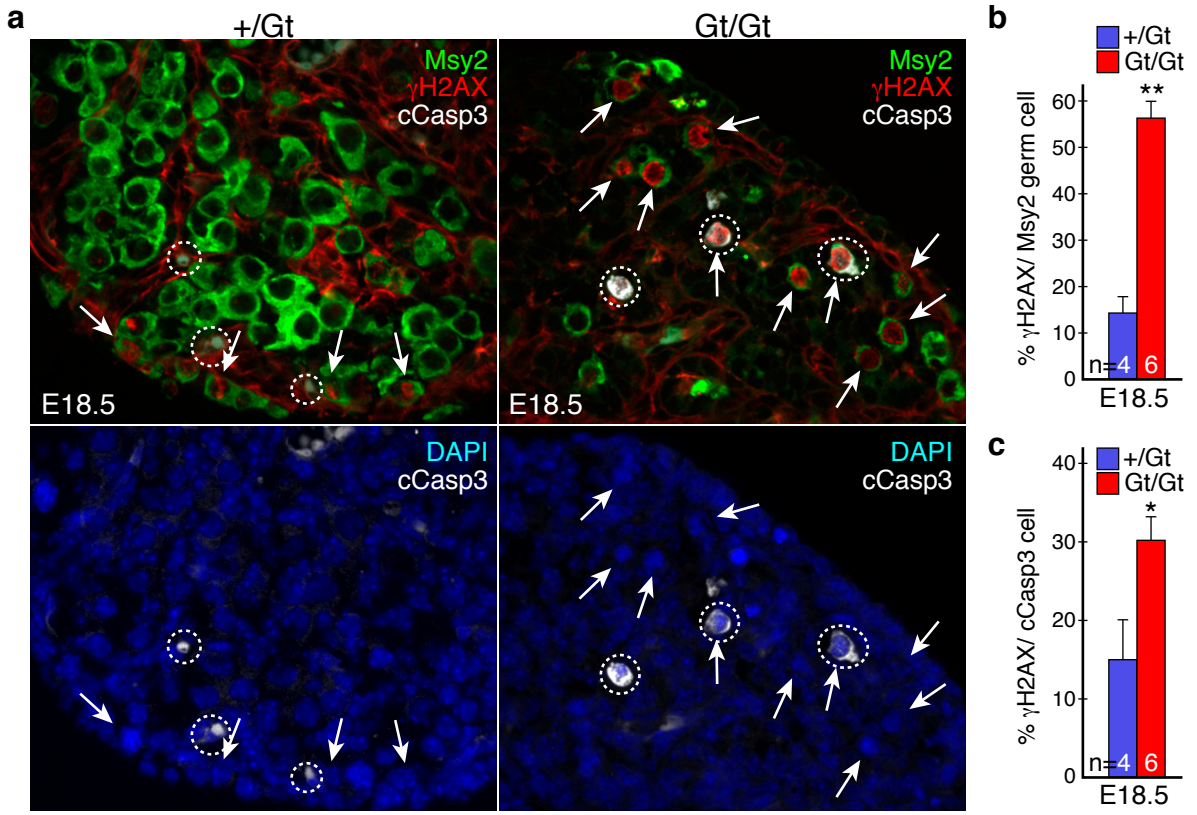

Figure S10. Unrepaired DSB in meiotic oocytes is associated with apoptotic cell death in Tet1$^{Gt/Gt}$ oocytes

(a) Representative images of Tet1$^{+/Gt}$ and Tet1$^{Gt/Gt}$ E18.5 ovary sections stained with γH2AX, Msy2, and cleaved Caspase3 (cCasp3). Arrows indicate γH2AX-positive cells, and dashed circles indicate cCasp3-positive cells.

(b) Percentage of γH2AX-positive cells in Msy2-posoitive cells in Tet1$^{+/Gt}$ and Tet1$^{Gt/Gt}$ E18.5 ovaries. Error bar indicates SEM. n=4-6. **P<0.01.

(c) Percentage of γH2AX-positive cells in cCasp3-posoitive cells in Tet1$^{+/Gt}$ and Tet1$^{Gt/Gt}$ E18.5 ovaries. Error bar indicates SEM. n=4-6. *P<0.05.

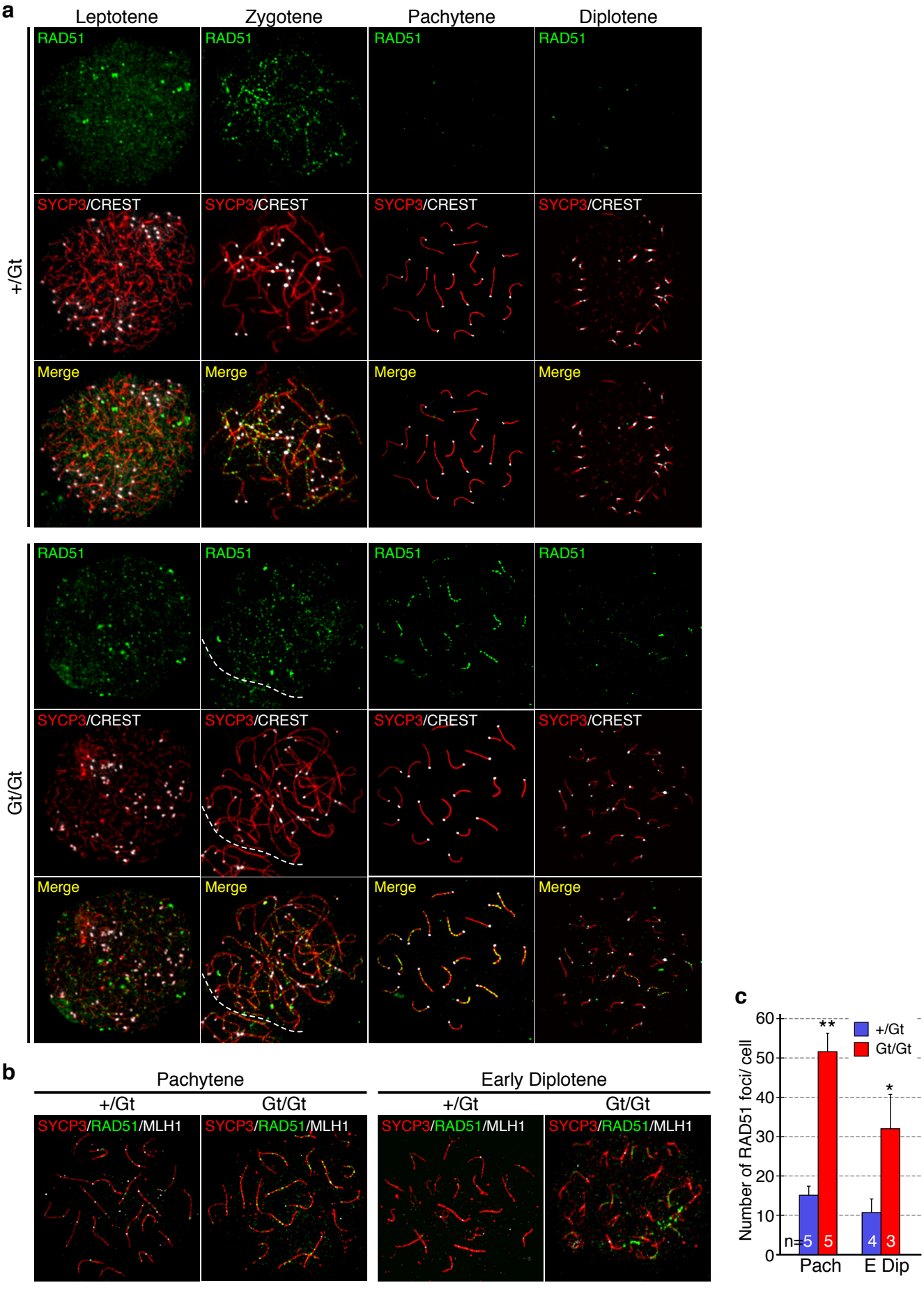
a
Leptotene
Zygotene
Pachytene
Diplotene
+/Gt
Gt/Gt
RAD51
SYCP3/CREST
Merge
b
Pachytene
Early Diplotene
+/Gt
Gt/Gt
SYCP3/RAD51/MLH1
c
Number of RAD51 foci/ cell
+/Gt
Gt/Gt
n=5
5
4
3
Pach
E Dip
**
*

Figure S11. Accumulation of RAD51-foci in pachytene Tet1$^{Gt/Gt}$ oocytes
(a) Representative images of Tet1$^{+/Gt}$ and Tet1$^{Gt/Gt}$ meiotic oocytes stained with RAD51, SYCP3, and CREST.
(b) Representative images of pachytene and early diplotene Tet1$^{+/Gt}$ and Tet1$^{Gt/Gt}$ oocytes stained with SYCP3, RAD51, and MLH1.
(c) The average number of RAD51-positive foci in pachytene and diplotene stage Tet1$^{+/Gt}$ and Tet1$^{Gt/Gt}$ oocytes. Error bars indicate SEM. n=3-5. *P<0.05, **P<0.01.

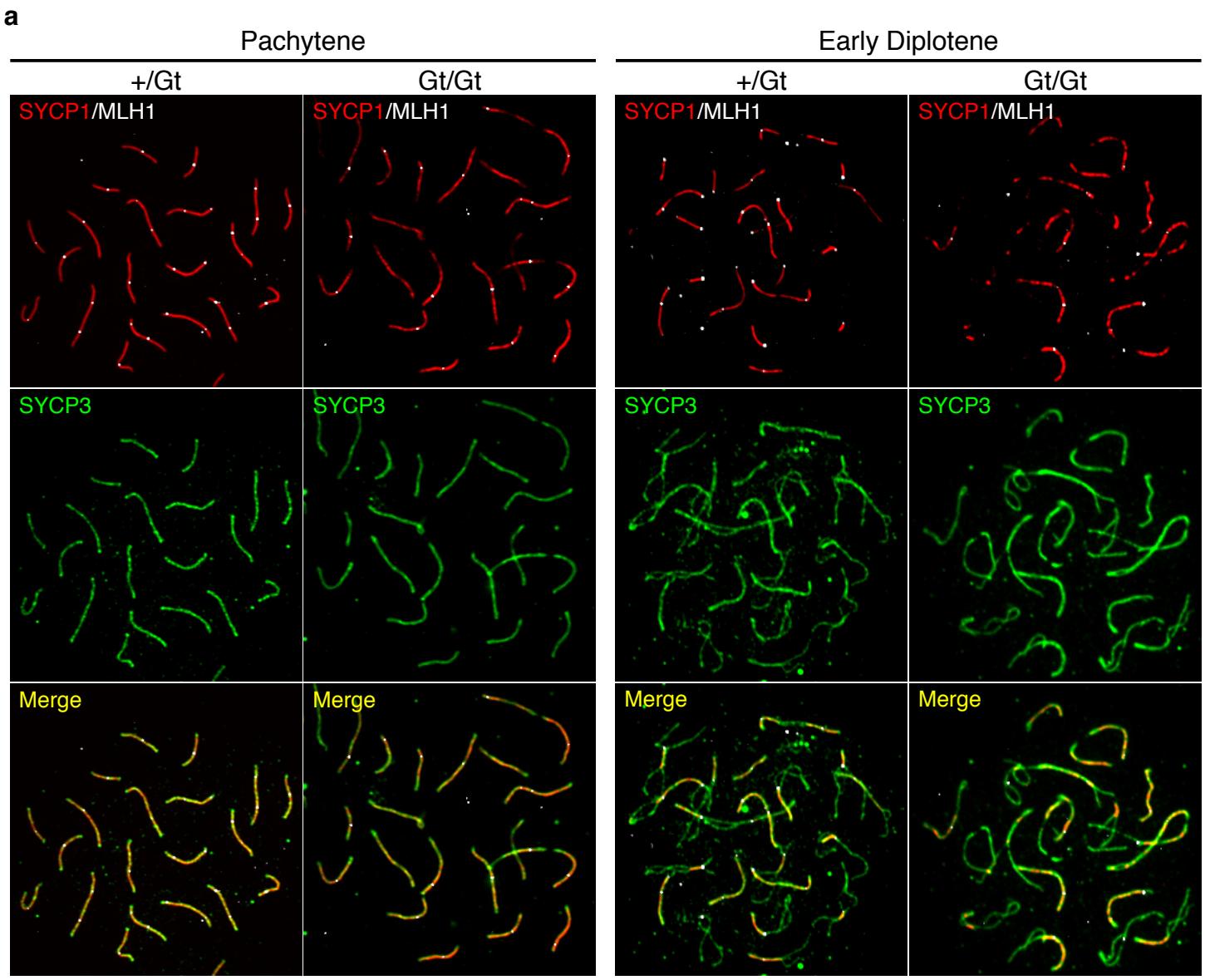

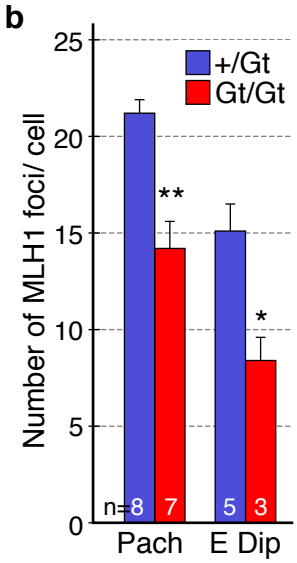

Figure S12. Significant decrease in crossover formation in Tet1Gt/Gt oocytes

(a) Representative images of pachytene and early diplotene stage Tet1$^{+/Gt}$ and Tet1$^{Gt/Gt}$ oocytes stained with SYCP1, MLH1, and SYCP3.

(b) The average number of MLH1-foci in pachytene and early diplotene stage Tet1$^{+/Gt}$ and Tet1$^{Gt/Gt}$ oocytes. Error bars indicate SEM. n=3-8. *P<0.05, **P<0.01.

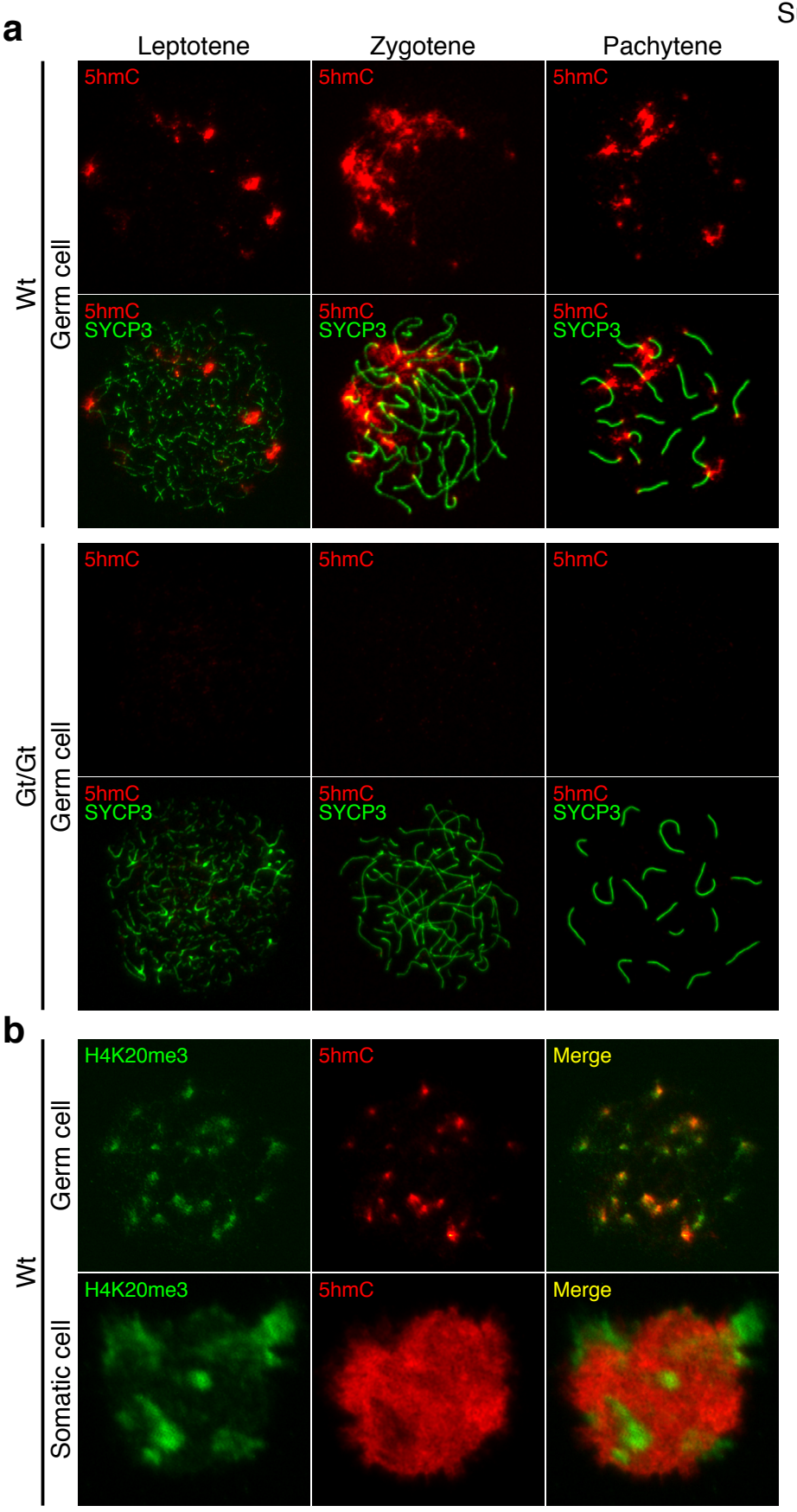

Figure S13. Loss of PCH enrichment of 5hmC in Tet1$^{Gt/Gt}$ oocytes
(a) Representative images of meiotic Tet1$^{+/Gt}$ and Tet1$^{Gt/Gt}$ oocytes co-stained with SYCP3 (green) and 5hmC (red) antibodies.
(b) Representative images of pachytene stage Wt oocytes and surrounding somatic cell co-stained with pericentric heterochromatin marker, H4K20me3 (green) and 5hmC (red) antibodies.

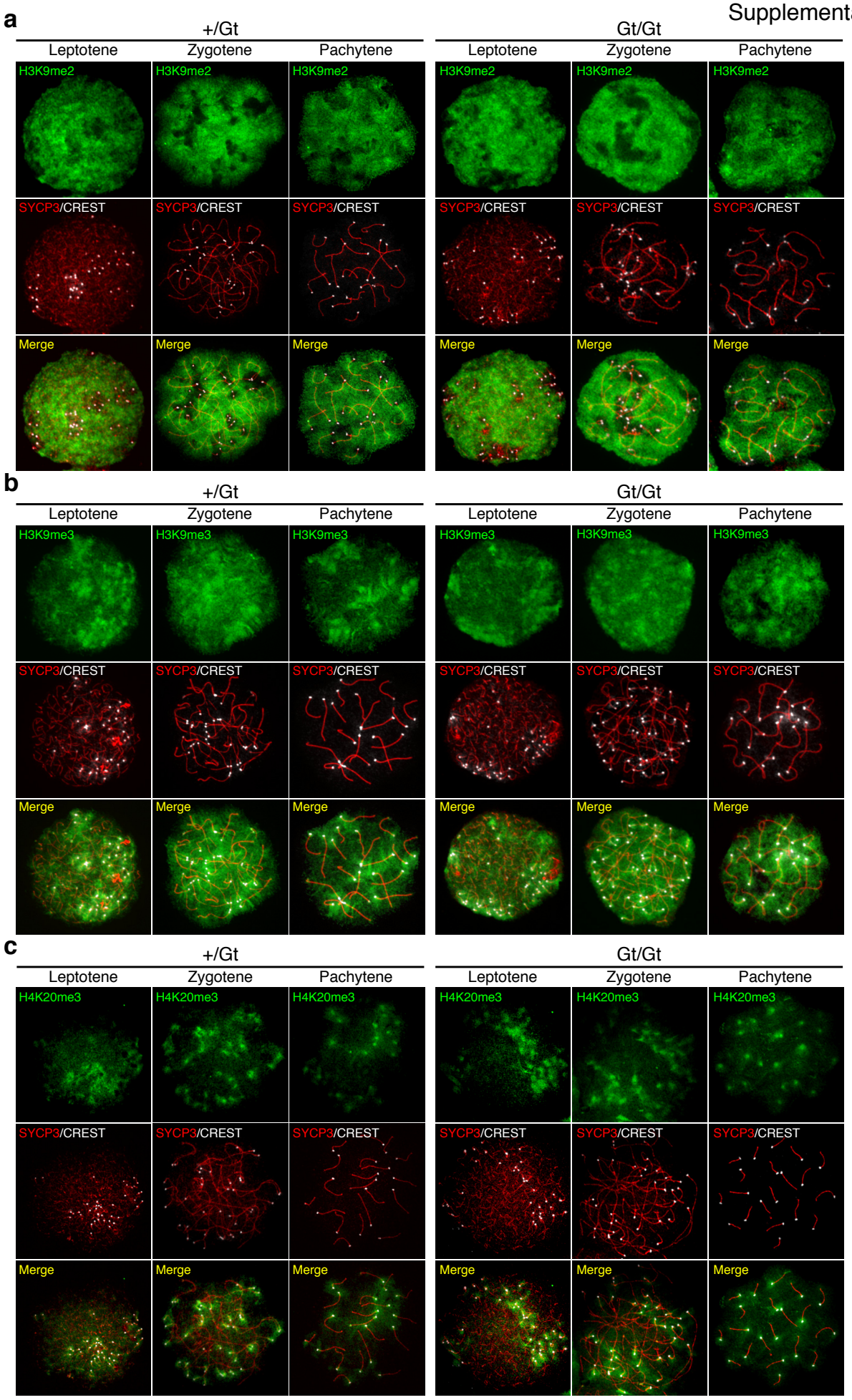
a
+/Gt
Gt/Gt
Leptotene
Zygotene
Pachytene
H3K9me2
SYCP3/CREST
Merge
b
+/Gt
Gt/Gt
Leptotene
Zygotene
Pachytene
H3K9me3
SYCP3/CREST
Merge
c
+/Gt
Gt/Gt
Leptotene
Zygotene
Pachytene
H4K20me3
SYCP3/CREST
Merge

Figure S14. No significant change in H3K9me2, H3K9me3, and H4K20me3 staining patterns in PCH of Tet1$^{Gt/Gt}$ oocytes

Representative images of meiotic Tet1$^{+/Gt}$ and Tet1$^{Gt/Gt}$ oocytes stained with H3K9me2 (a), H3K9me3 (b), and H4K20me3 (c). SC and PCH are marked by SYCP3 (red) and CREST (white), respectively.

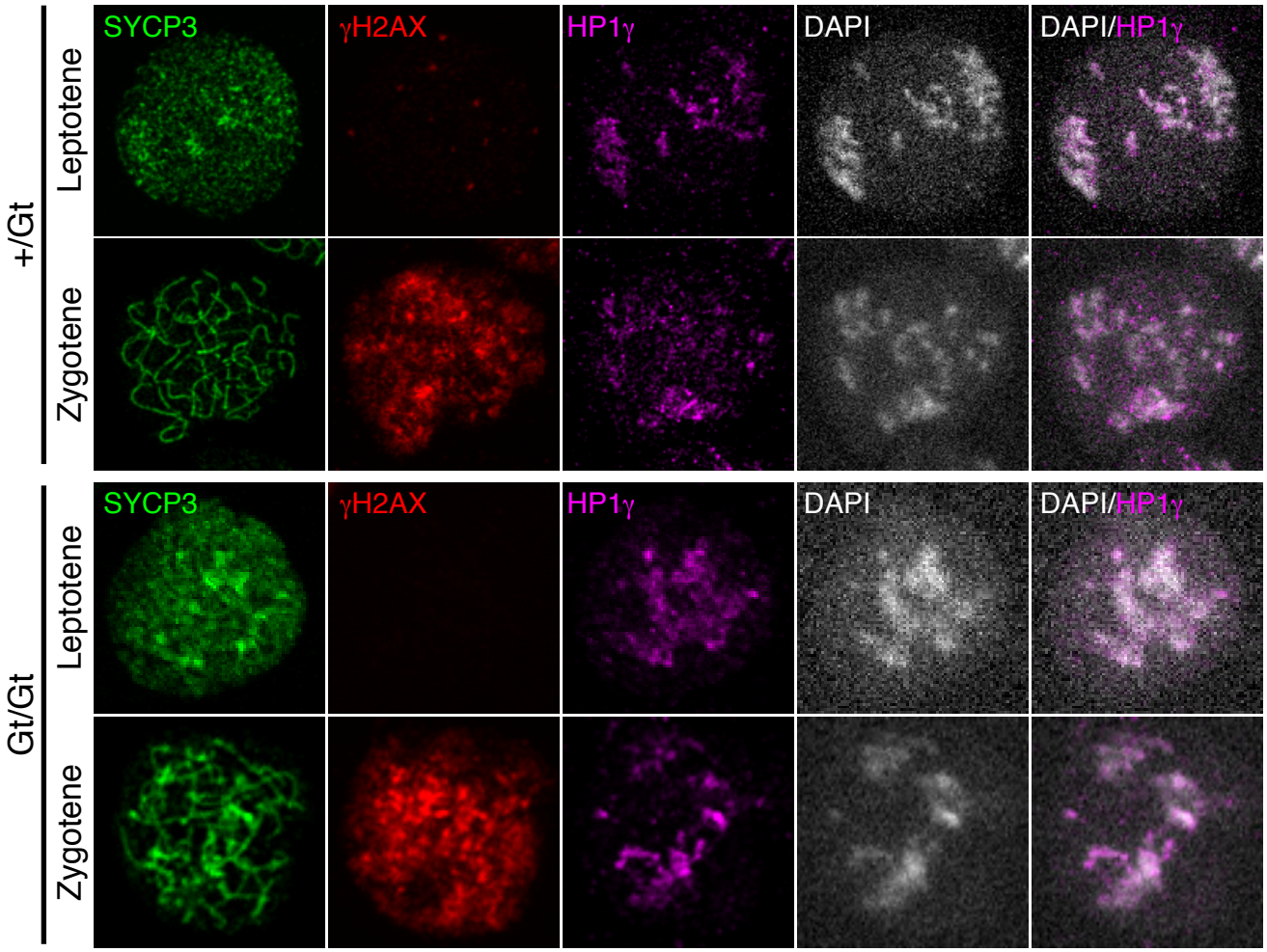

Figure S15. No significant change in HP1γ staining pattern in Tet1$^{Gt/Gt}$ oocytes
Representative image of zygotene and leptotene Tet1$^{+/Gt}$ and Tet1$^{Gt/Gt}$ oocytes stained with HP1γ antibodies.

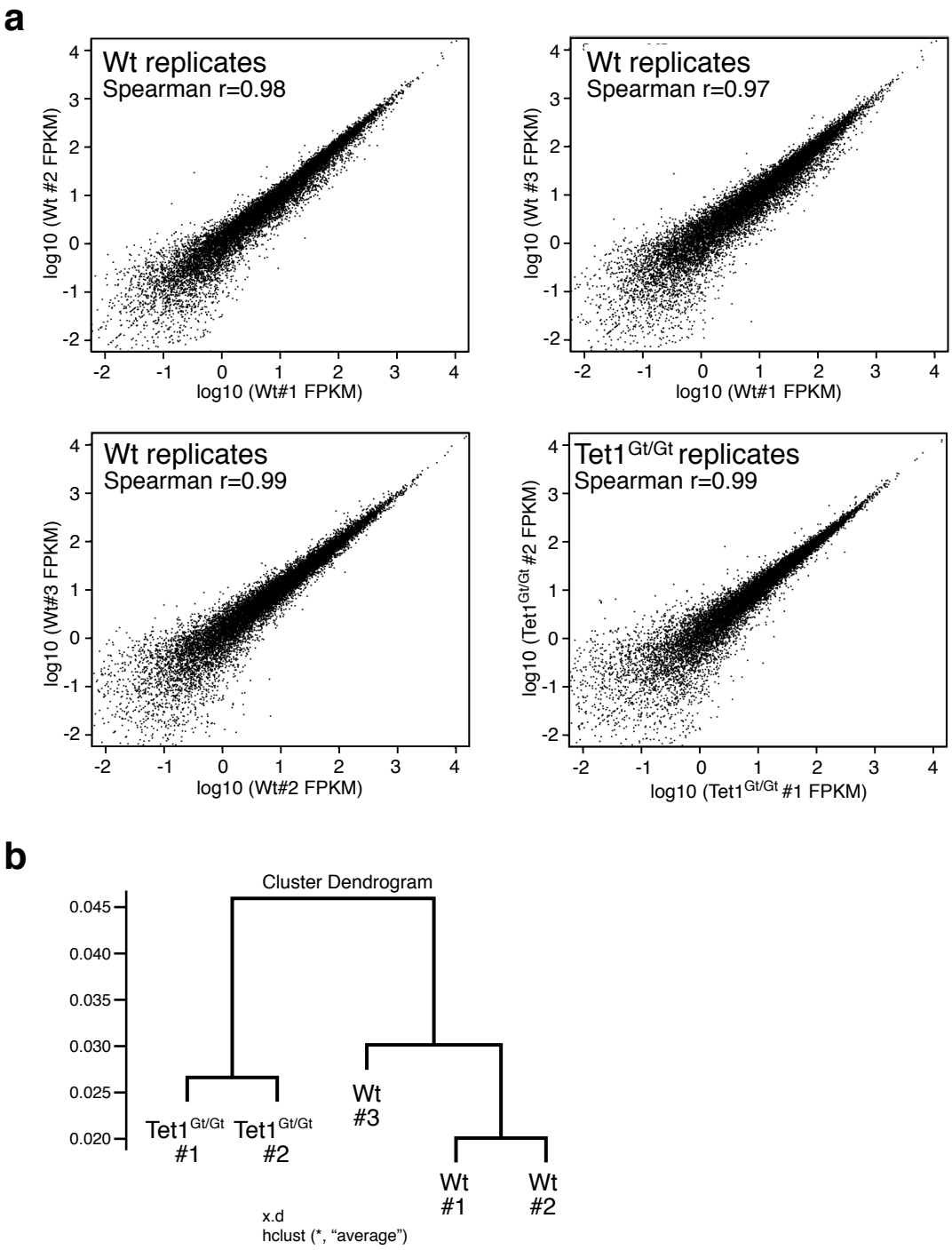

Figure S16. Biological replicates of RNA-seq data is highly reproducible
(a) Correlation of RNA-seq data from replicates in Wt and Tet1$^{Gt/Gt}$ E13.5 female PGCs.
(b) Hierarchical clustering of all samples from Wt and Tet1$^{Gt/Gt}$ E13.5 female PGCs.

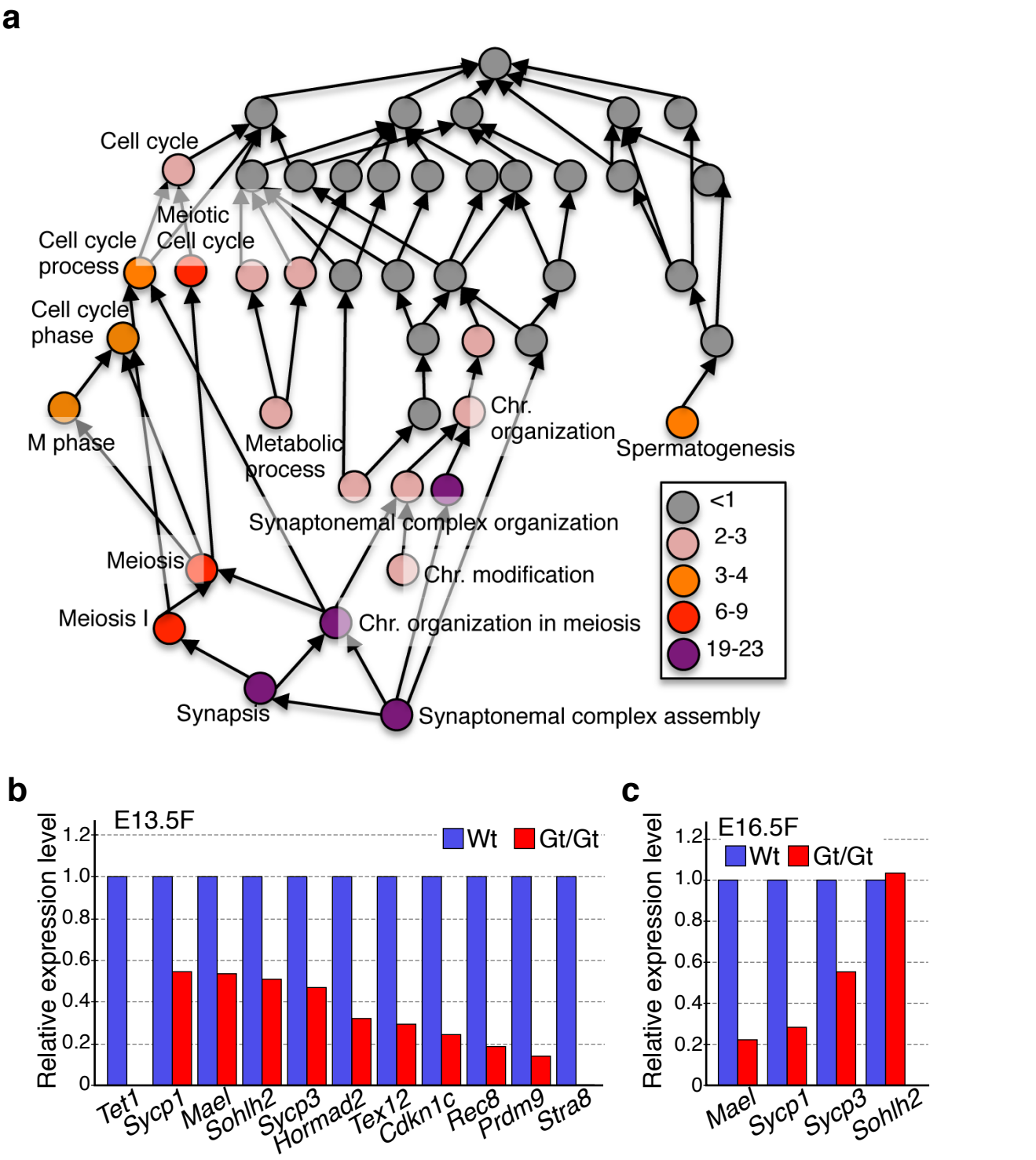

Figure S17. Alteration of meiotic genes in Tet1$^{Gt/Gt}$ E13.5 female PGCs
(a) Local directed acyclic graph for enriched GO terms of biological process. Nodes are colore-coded according to binomial fold enrichment.
(b, c) RT-qPCR verification of the down-regulated meiotic genes in E13.5 (b) or E16.5 (c) female germ cells. To avoid biased amplification, purified germ and somatic cells from three embryos of each genotype were combined and analyzed. The expression level in wild-type PGCs is set as 1.

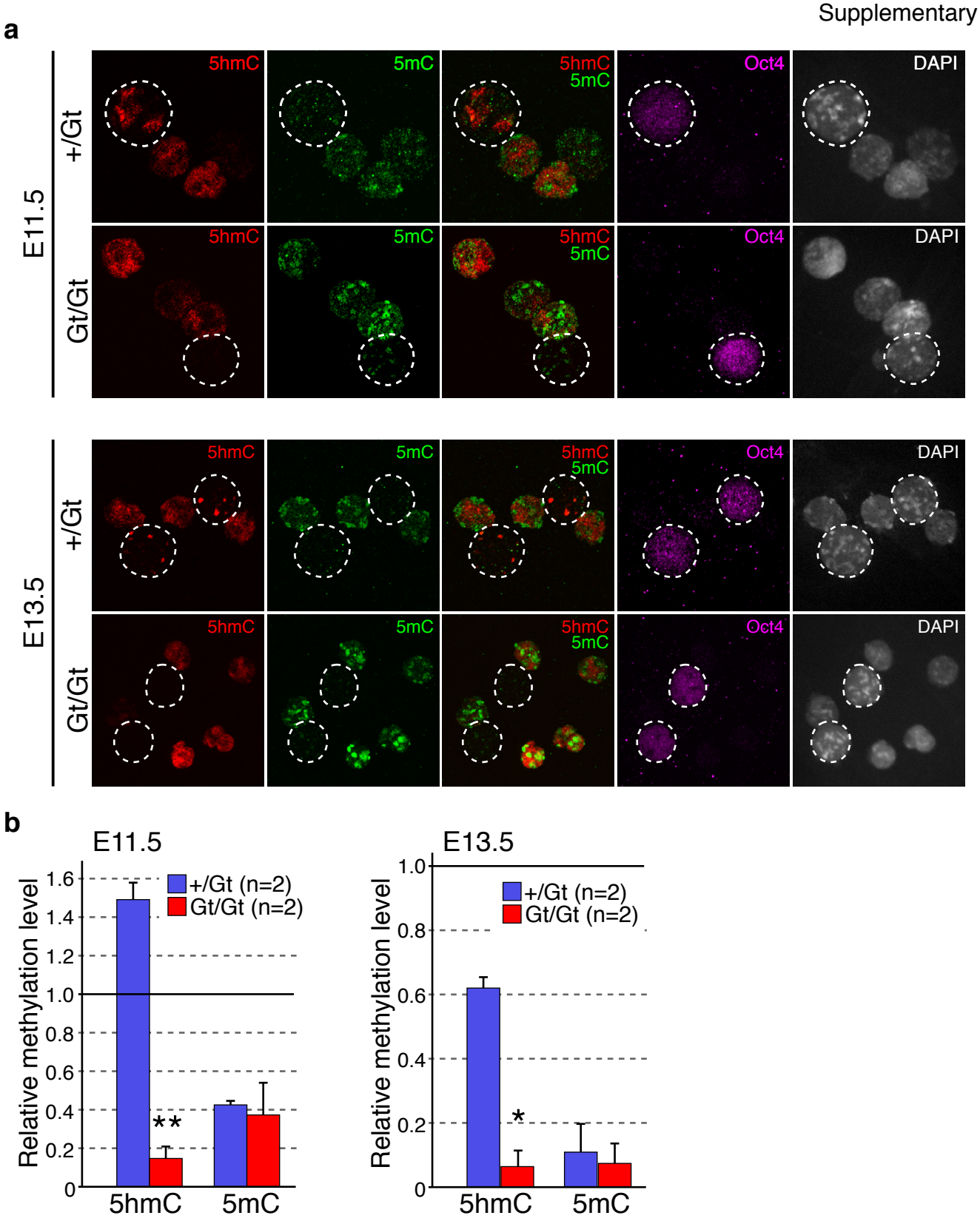

Figure S18. Effects of Tet1 depletion on global 5mC and 5hmC levels assayed by immunostaining
(a) Representative images of immunocytochemistry of E11.5 and E13.5 Tet1$^{+/Gt}$ and Tet1$^{Gt/Gt}$ PGC spreads stained with 5hmC and 5mC antibodies. Dashed circles indicate PGCs.
(b) Relative signal intensity of 5hmC and 5mC to somatic cells. Signal intensity of PGC was calculated with software and normalized with the average value of two neighboring somatic cells of the same image. Average value of each genotype was calculated from 20-25 PGCs. Error bar indicates SEM. n=2. *P<0.05. **P<0.01.

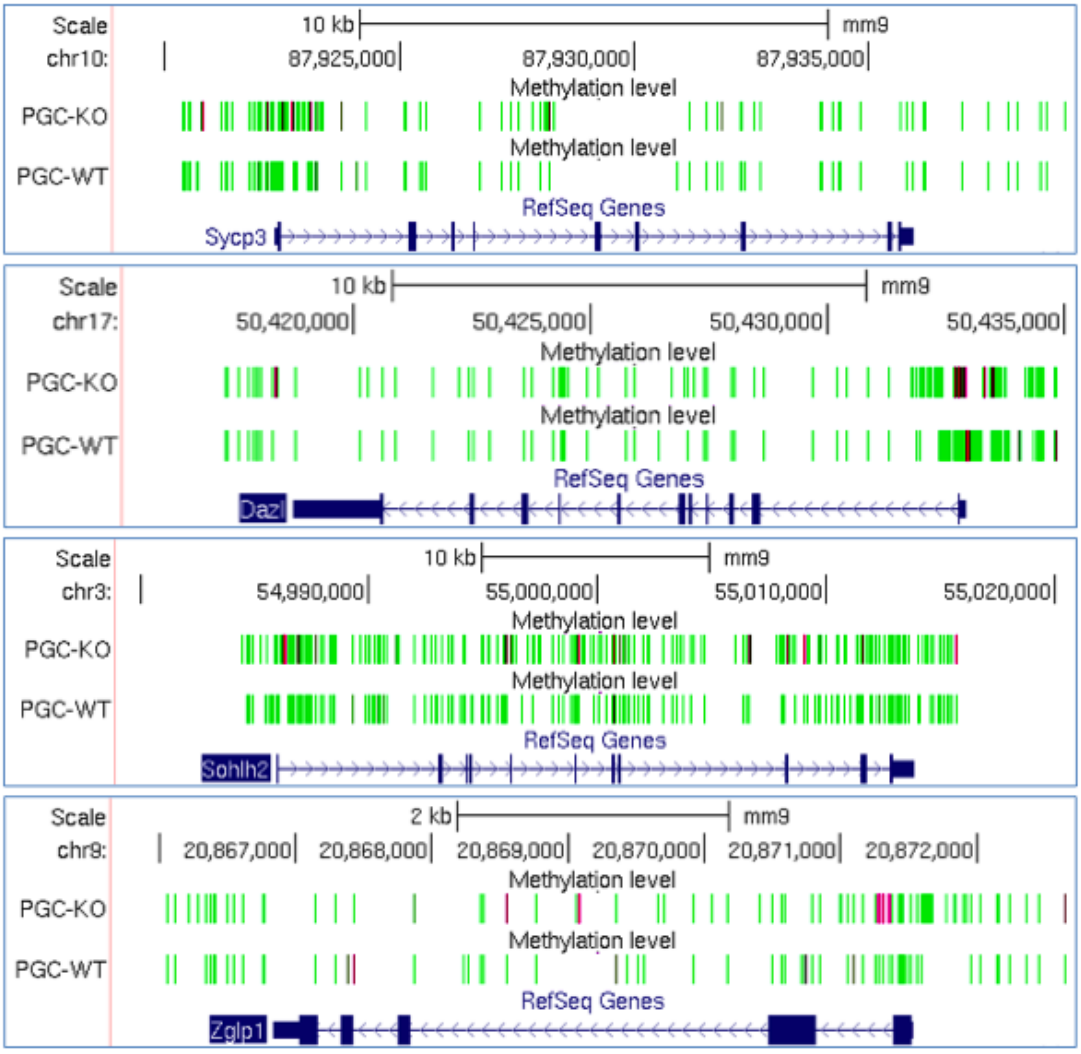

Figure S19. Examples of differentially expressed genes associated with DMR
Green bars indicate unmethylated CpGs, red bars indicate methylated CpGs.

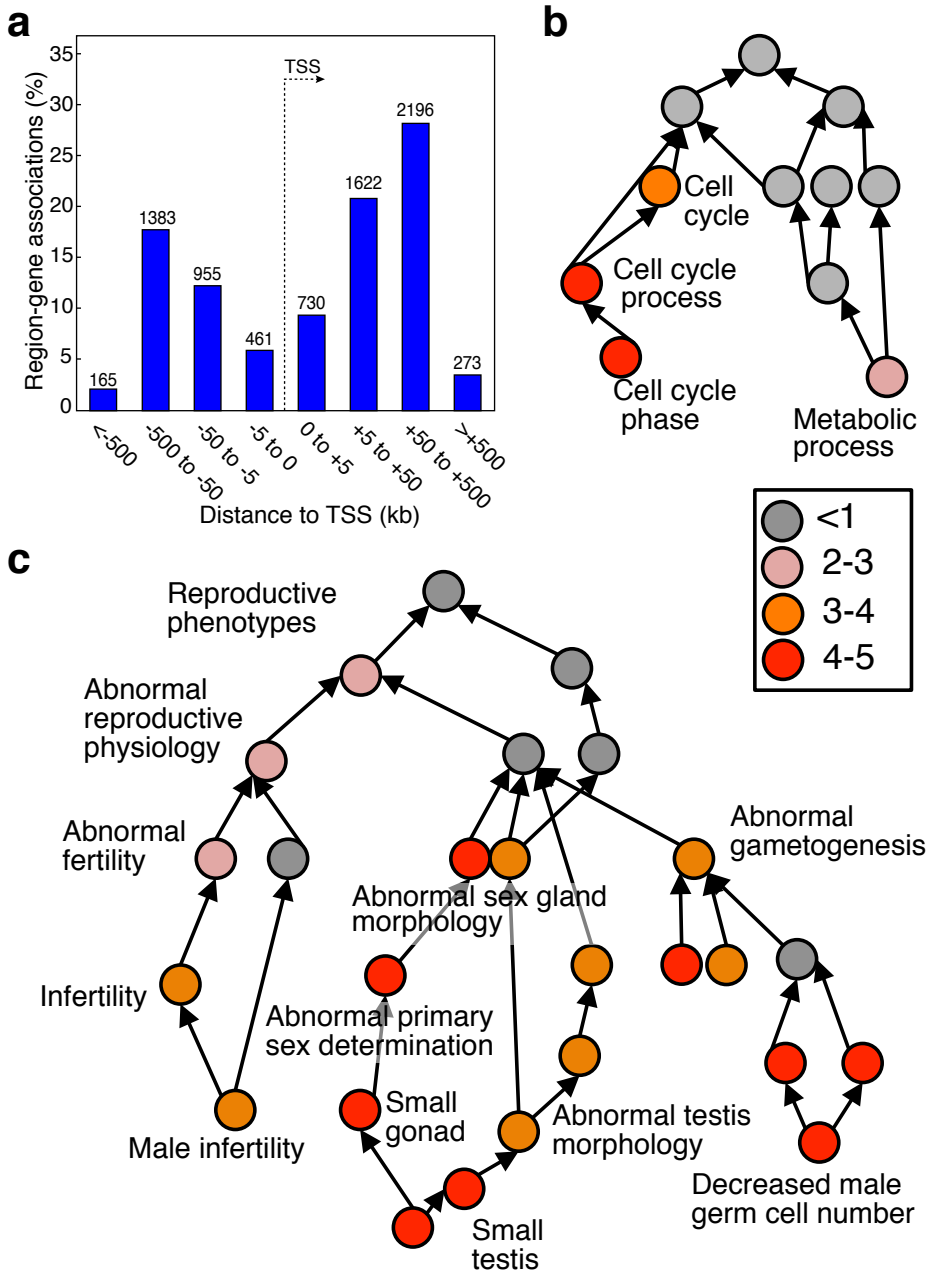

Figure S20. Distribution and gene ontology analysis of DMRs
(a) The location of differentially methylated regions (DMRs) related to transcription start site. The DMRs between Tet1$^{Gt/Gt}$ and wild-type PGCs are mostly located far away from the transcriptional start sites.
(b, c) GO terms related with cell cycle process (b) and mouse phenotypes associated with reproductive abnormalities (c) were enriched for the 255 differentially expressed and DMR associated genes in Tet1$^{Gt/Gt}$. Local directed acyclic graphs were modified from GREAT ontology visualizer in that nodes are color-coded according to binomial fold enrichment.